

Tunable and highly sensitive temperature sensor based on graphene photonic crystal fiber

Xu Cheng(程旭), Xu Zhou(周旭), Chen Huang(黄琛), Can Liu(刘灿), Chaojie Ma(马超杰), Hao Hong(洪浩), Wentao Yu(于文韬), Kaihui Liu(刘开辉), and Zhongfan Liu(刘忠范)

Citation: Chin. Phys. B, 2021, 30 (**11**): 118103. DOI: 10.1088/1674-1056/ac11d0
Journal homepage: http://cpb.iphy.ac.cn; http://iopscience.iop.org/cpb

What follows is a list of articles you may be interested in

Direct growth of graphene films without catalyst on flexible glass substrates by PECVD

Rui-Xia Miao(苗瑞霞), Chen-He Zhao(赵晨鹤), Shao-Qing Wang(王少青), Wei Ren(任卫), Yong-Feng Li(李永锋), Ti-Kang Shu(束体康), and Ben Yang(杨奔)

Chin. Phys. B, 2021, 30 (**9**): 098101. DOI: 10.1088/1674-1056/abeeec

Intercalation of germanium oxide beneath large-area and high-quality epitaxial graphene on Ir(111) substrate

Xueyan Wang(王雪艳), Hui Guo(郭辉), Jianchen Lu(卢建臣), Hongliang Lu(路红亮), Xiao Lin(林晓), Chengmin Shen(申承民), Lihong Bao(鲍丽宏), Shixuan Du(杜世萱), and Hong-Jun Gao(高鸿钧)

Chin. Phys. B, 2021, 30 (**4**): 048102. DOI: 10.1088/1674-1056/abe22c

A review of experimental advances in twisted graphene moirè superlattice

Yanbang Chu(褚衍邦), Le Liu(刘乐), Yalong Yuan(袁亚龙), Cheng Shen(沈成), Rong Yang(杨蓉), Dongxia Shi(时东霞), Wei Yang(杨威), and Guangyu Zhang(张广宇)

Chin. Phys. B, 2020, 29 (**12**): 128104. DOI: 10.1088/1674-1056/abb221

Epitaxial synthesis and electronic properties of monolayer Pd_2Se_3

Peng Fan(范朋), Rui-Zi Zhang(张瑞梓), Jing Qi(戚竞), En Li(李恩), Guo-Jian Qian(钱国健), Hui Chen(陈辉), Dong-Fei Wang(王东飞), Qi Zheng(郑琦), Qin Wang(汪琴), Xiao Lin(林晓), Yu-Yang Zhang(张余洋), Shixuan Du(杜世萱), Hofer W A, Hong-Jun Gao(高鸿钧)

Chin. Phys. B, 2020, 29 (**9**): 098102. DOI: 10.1088/1674-1056/abab80

High sensitive pressure sensors based on multiple coating technique

Rizwan Zahoor, Chang Liu(刘畅), Muhammad Rizwan Anwar, Fu-Yan Lin(林付艳), An-Qi Hu(胡安琪), Xia Guo(郭霞)

Chin. Phys. B, 2020, 29 (**2**): 028102. DOI: 10.1088/1674-1056/ab6721

RAPID COMMUNICATION

Tunable and highly sensitive temperature sensor based on graphene photonic crystal fiber*

Xu Cheng(程旭)[1], Xu Zhou(周旭)[2,3], Chen Huang(黄琛)[1], Can Liu(刘灿)[1], Chaojie Ma(马超杰)[1], Hao Hong(洪浩)[1], Wentao Yu(于文韬)[1,‡], Kaihui Liu(刘开辉)[1,4,†], and Zhongfan Liu(刘忠范)[3,5,§]

[1] *State Key Laboratory for Mesoscopic Physics, Frontiers Science Center for Nano-optoelectronics, School of Physics, Peking University, Beijing* 100871, *China*

[2] *Guangdong Provincial Key Laboratory of Quantum Engineering and Quantum Materials, School of Physics and Telecommunication Engineering, South China Normal University, Guangzhou* 510006, *China*

[3] *Beijing Graphene Institute (BGI), Beijing* 100095, *China*

[4] *International Centre for Quantum Materials, Collaborative Innovation Center of Quantum Matter, Beijing* 100871, *China*

[5] *Center for Nanochemistry, College of Chemistry and Molecular Engineering, Peking University, Beijing* 100871, *China*

(Received 10 June 2021; revised manuscript received 25 June 2021; accepted manuscript online 7 July 2021)

Optical fiber temperature sensors have been widely employed in enormous areas ranging from electric power industry, medical treatment, ocean dynamics to aerospace. Recently, graphene optical fiber temperature sensors attract tremendous attention for their merits of simple structure and direct power detecting ability. However, these sensors based on transfer techniques still have limitations in the relatively low sensitivity or distortion of the transmission characteristics, due to the unsuitable Fermi level of graphene and the destruction of fiber structure, respectively. Here, we propose a tunable and highly sensitive temperature sensor based on graphene photonic crystal fiber (Gr-PCF) with the non-destructive integration of graphene into the holes of PCF. This hybrid structure promises the intact fiber structure and transmission mode, which efficiently enhances the temperature detection ability of graphene. From our simulation, we find that the temperature sensitivity can be electrically tuned over four orders of magnitude and achieve up to $\sim 3.34 \times 10^{-3}$ dB/(cm·°C) when the graphene Fermi level is ~ 35 meV higher than half the incident photon energy. Additionally, this sensitivity can be further improved by ~ 10 times through optimizing the PCF structure (such as the fiber hole diameter) to enhance the light–matter interaction. Our results provide a new way for the design of the highly sensitive temperature sensors and broaden applications in all-fiber optoelectronic devices.

Keywords: graphene, photonic crystal fiber, temperature sensor, high sensitivity, Fermi level

PACS: 81.05.ue, 78.67.–n, 07.07.Df, 42.70.Gi **DOI:** 10.1088/1674-1056/ac11d0

Optical fiber, as one of the most remarkable waveguides, possesses many intrinsic excellent features such as ultralow transmission loss, perfect single-mode transmission ability, anti-electromagnetic interference capacity and the compatibility for complex environments.[1–4] These characteristics have made it an attractive platform for all-fiber temperature sensors, which are widely used in applications such as fire monitoring, temperature distribution of engines, and magnetic resonance imaging.[5–7] Traditional optical fiber temperature sensors are mainly based on fiber gratings or interferometers, in which the environment temperature change leads to the variation of the grating pitch or the optical path difference in interferometers, and results in the change of the detecting signal. However, these fiber temperature sensors suffer from complicated structural design and wavelength resolved measurement system.[8–10] To break through this dilemma, some strategies have been developed, including combining optical fiber with functional thermo-sensitive materials.[11–13]

Originating from the atom-scale hexagonal lattice structure and unique Dirac band, graphene has exhibited exceptional electrical, optical and thermal properties.[14–23] Herein, the tunable light absorption ability under different environment temperatures endows graphene with the potential to sense temperature via simple sensor construction and direct power detecting system.[24–27] Considering atomic thickness of graphene and light–matter interaction enhancement capacity of optical fiber, it is mutually beneficial to integrate both for all-fiber temperature sensors. In the current manufac-

*Project supported by the National Natural Science Foundation of China (Grant Nos. 52021006, 52025023, 51991342, and 11888101), the Key R&D Program of Guangdong Province, China (Grant Nos. 2019B010931001, 2020B010189001, and 2018B030327001), the Pearl River Talent Recruitment Program of Guangdong Province, China (Grant No. 2019ZT08C321), the Strategic Priority Research Program of Chinese Academy of Sciences (Grant No. XDB33000000), Beijing Natural Science Foundation, China (Grant No. JQ19004), Beijing Municipal Science & Technology Commission, China (Grant No. Z181100004818003), the China Postdoctoral Science Foundation (Grant No. 2020M680177), National Postdoctoral Program for Innovative Talents of China (Grant No. BX20190016), and China Postdoctoral Science Foundation (Grant No. 2019M660280).

†Corresponding author. E-mail: khliu@pku.edu.cn

‡Corresponding author. E-mail: wtyu@pku.edu.cn

§Corresponding author. E-mail: zfliu@pku.edu.cn

© 2021 Chinese Physical Society and IOP Publishing Ltd

ture technologies, side-polished and tapered optical fibers are most commonly used platforms to combine with graphene due to the evanescent wave coupling. However, these temperature sensors based on transfer techniques conventionally suffer from the distortion of the propagation mode or short interaction length with relatively low sensitivity,[28–33] which limit their practical applications. Besides, the influences of the Fermi level (E_F) variation on light absorbance of graphene and the consequent sensor performance are still unclear, which may be a key point to further improve the sensitivity of the temperature sensors.[34]

Here, we propose a highly sensitive temperature sensor based on graphene photonic crystal fiber (Gr-PCF) (Fig. 1(a)), in which the transmission mode is kept intact and the intensity of the transmitted light changes with temperature. Technically, the Gr-PCF can be massively fabricated by direct chemical vapor deposition method,[35] which endows it with the great potential in the practical application as a temperature sensor. This all-fiber temperature sensor theoretically exhibits a tunable sensitivity by modulating graphene E_F, and the highest sensitivity can reach $\sim 3.34 \times 10^{-3}$ dB/(cm·°C) with $E_F = 0.435$ eV under 1550 nm incident photon (~ 0.8 eV), dramatically enhanced compared with that at charge neutral point. Through optimizing the PCF structure, the sensitivity can be further enhanced by 10 times to 0.036 dB/(cm·°C). Our results provide a promising new way for high-performance all-fiber temperature sensors based on Gr-PCF.

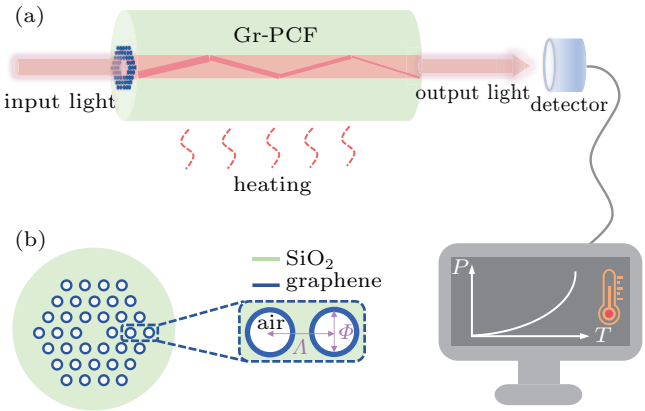


Fig. 1. Schematic illustration of Gr-PCF temperature sensor. (a) The configuration of Gr-PCF temperature sensor, in which the change of environment temperature can be monitored by the change of output light power. (b) Schematic of Gr-PCF cross-section, where graphene film is fully covered on the inner surface of air holes in PCF cladding (the hole diameter Φ and pitch Λ are both at micron scale).

In the as-designed Gr-PCF temperature sensor, a graphene film is attached tightly on the hole surface in PCF, where the PCF structure is selected according to the commercial one based on the total internal reflection theory for the practical application potential. In the cross-section of Gr-PCF, six circles of air holes are arranged periodically in the PCF cladding with the hole diameter (Φ) of 2.22 μm and pitch (Λ) of 5.4 μm (Fig. 1(b), 3 circles of air holes just for schematic diagram). Besides, the diameters of the solid core and the whole optical fiber are ~ 8.6 and ~ 125 μm, respectively. The selected PCF structure guarantees the endless single-mode property and low insertion loss with commercial single-mode fiber at the operating wavelength near 1550 nm.[36] The characterizations of the light distribution and transmission attenuation in the Gr-PCF at different temperatures are obtained by full-vector finite element simulation method.[37–40] As shown in the electric field distribution of the fundamental mode in Gr-PCF and the bare fiber, the addition of atomic thickness graphene film does not distort the propagation mode, which indicates the perfect integration ability of graphene and photonic crystal fiber (Figs. S1(a) and S1(b)). The propagating light in this fiber can continuously interact with the graphene film along the axis of the fiber via the evanescent wave coupling (Fig. S1(c)), which leads to the strong light–matter interaction.

The mechanism of this Gr-PCF temperature sensor is directly related to the Fermi–Dirac distribution change of the electrons in graphene with temperature at a given E_F such as the charge neutral point (Fig. 2(a)). At the temperature of 0 K, the electrons are entirely distributed under E_F (Fig. 2(a), left panel). Then with the temperature arising ($T > 0$ K), some electrons possess larger kinetic energy and occupy higher energy levels above E_F[41] (Fig. 2(a), right panel). Hence, the temperature change contributes to the electron redistribution in the Dirac-cone energy band of graphene and further results in the variation of its conductivity (σ_{Gr}) according to the Kubo formula, which is directly related to the complex refractive index (n_{Gr}):[25–27]

$$\begin{aligned}&\sigma_{Gr}(\omega, E_F, \Gamma, T)\\ &= -\frac{ie^2(\omega+2i\Gamma)}{\pi\hbar^2}\\ &\quad\times\left[\frac{1}{(\omega+2i\Gamma)^2}\int_0^\infty d\varepsilon\left(\frac{\partial n_F(\varepsilon)}{\partial\varepsilon}-\frac{\partial n_F(-\varepsilon)}{\partial\varepsilon}\right)\varepsilon\right.\\ &\quad\left.-\int_0^\infty d\varepsilon\left(\frac{n_F(-\varepsilon)-n_F(\varepsilon)}{(\omega+2i\Gamma)^2-4(\varepsilon/\hbar)^2}\right)\right],\end{aligned} \tag{1}$$

$$n_{Gr} = n+ik = \sqrt{\varepsilon_{Gr}} = \sqrt{1+\frac{i\sigma_{Gr}}{\varepsilon_0\omega d_{Gr}}}, \tag{2}$$

where $n_F(\varepsilon) = 1/\{1+\exp[(\varepsilon-E_F)/(k_BT)]\}$ is Fermi–Dirac distribution, ε is the electron energy, k_B is the Boltzmann constant, T is the temperature, ω is the radian frequency, Γ is the scattering rate, $\hbar$ is the reduced Planck's constant, ε_0 is the vacuum permittivity, and d_{Gr} is the graphene thickness. At the condition of $E_F = 0$ eV and 1550 nm incident light, the imaginary part (k) of n_{Gr} shows a decreasing trend with temperature rising from −100 °C to 100 °C, leading to the decrease of graphene absorption (Fig. 2(b)). Meanwhile, the real

part (n) of n_{Gr} increases with temperature (Fig. 2(c)), bringing about the increase of the refractive index in fiber cladding and consequent enhancement of the normalized light intensity I (ratio of intensity at the innermost graphene position to that at the fiber core center) in Gr-PCF (Fig. 2(d)). Taking the combined influences of k and n into account, the change of transmission attenuation in Gr-PCF with the temperature from -100 °C to 100 °C is demonstrated as $\sim 6.4 \times 10^{-5}$ dB for one-centimeter-long fiber (Fig. 2(e)), which shows the enormous potential to monitor temperature through light intensity change.

Considering the unique and adjustable E_F characteristic of graphene, it is significant to modulate the E_F for optimizing the transmission attenuation and the sensitivity of the sensor. Therefore, we systematically investigate the influence of E_F on the performance of Gr-PCF temperature sensor, and find that the sensitivity can be highly improved when E_F is adjusted at a suitable level around 0.4 eV (half energy of the incident photon of 1550 nm, Fig. 3(a)). In this case, the transmission attenuation is much lower than that at the charge neutral point ($E_F = 0$ eV) and the difference of attenuations between -100 °C and 100 °C ($|\Delta A|$) drastically changes with E_F tuned around 0.4 eV, which indicates the possibility to enhance the sensitivity via tuning E_F (Fig. S2). This attenuation change with temperature results from the combined effects of k and n, which are related to the absorption of graphene and the light distribution at the innermost graphene film respectively and show an obvious change with E_F adjusted around 0.4 eV at different temperatures (Figs. 3(b) and 3(c)). In detail, the light transmission attenuation in Gr-PCF shows a decreasing trend with temperature from -100 °C to 100 °C with E_F in the range of 0.35 eV to 0.40 eV, but an increasing trend with E_F in the range of 0.40 eV to 0.45 eV (Fig. 3(d)). Besides, when E_F is adjusted from 0.3 eV to 0.45 eV, k and n vary from ~ 2.6 to ~ 0.4 and ~ 3.2 to ~ 2.2 at a constant temperature of 0 °C, respectively (Fig. S3), contributing the decreasing trend of the total transmission attenuation of Gr-PCF. For the practical sensor applications, it is important to obtain the high sensitivity with low total transmission attenuation by setting a suitable E_F. As a result, the $|\Delta A|$ shows a maximum ~ 0.668 dB/cm at $E_F = 0.435$ eV (four orders of magnitude improvement than that at 0 eV) with a relatively low attenuation compared to that at another peak position of $E_F = 0.365$ eV (Figs. 3(d) and 3(e)). This result also indicates $\sim 3.34 \times 10^{-3}$ dB/(cm·°C) sensitivity for temperature sensing, where the unit dB/(cm·°C) is used to describe temperature sensing ability of Gr-PCF for the unit fiber length. In principle, the absorption of graphene is directly dependent on the electron distribution at the energy level of half the incident photon energy (±0.4 eV for 1550 nm incident light). Hence, for the case of $E_F = 0.4$ eV, the distribution probability at 0.4 eV (the same as E_F) is always a constant 0.5, and that at -0.4 eV changes very slightly with temperature due to the large energy difference from E_F, which results in a very small attenuation fluctuation with temperature at $E_F = 0.4$ eV compared to that at $E_F = 0.435$ eV (Fig. 3(e)).

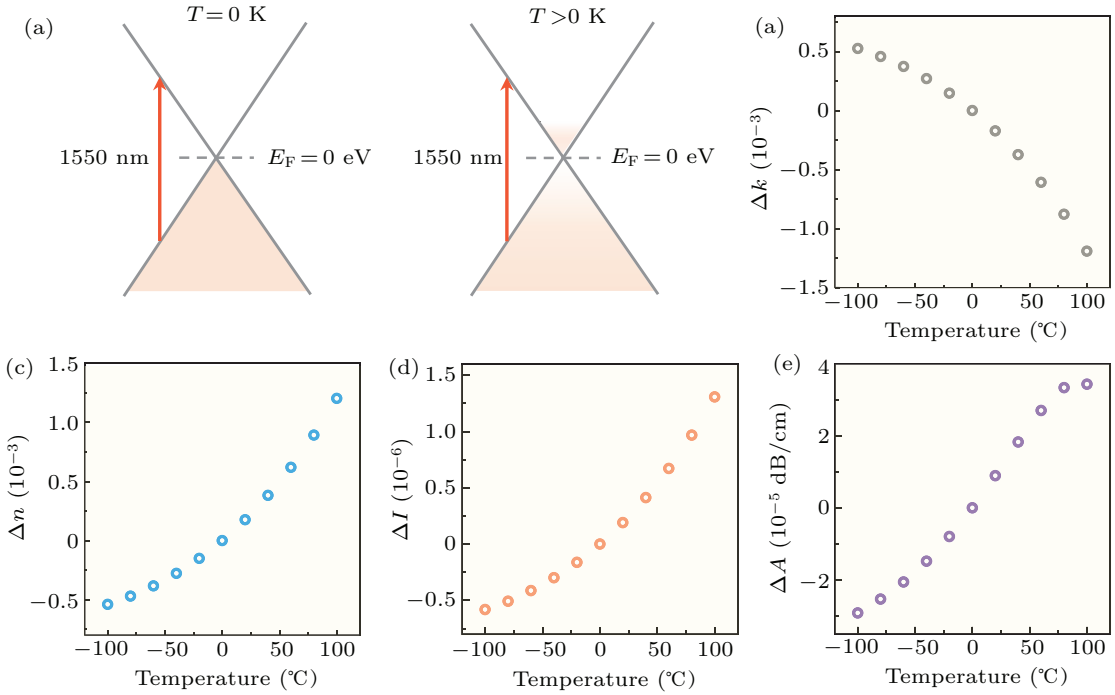


Fig. 2. Temperature sensing property of Gr-PCF with $E_F = 0$ eV. (a) Fermi–Dirac distributions of electrons in graphene at different temperatures, resulting in the changes of the conductivity and complex refractive index of graphene. (b)–(e) The relative changes of the imaginary part Δk (b) and real part Δn (c) of graphene complex refractive index, the relative normalized intensity (ratio of intensity at the innermost graphene position to that at the fiber core center) ΔI (d), and the relative attenuation ΔA (e) with temperatures from -100 °C to 100 °C. Here Δ represents difference between values at a given temperature and that at 0 °C, where k, n, I and A are 2.8326, 2.9340, 11.37467% and 4.04843 dB/cm at 0 °C, respectively.

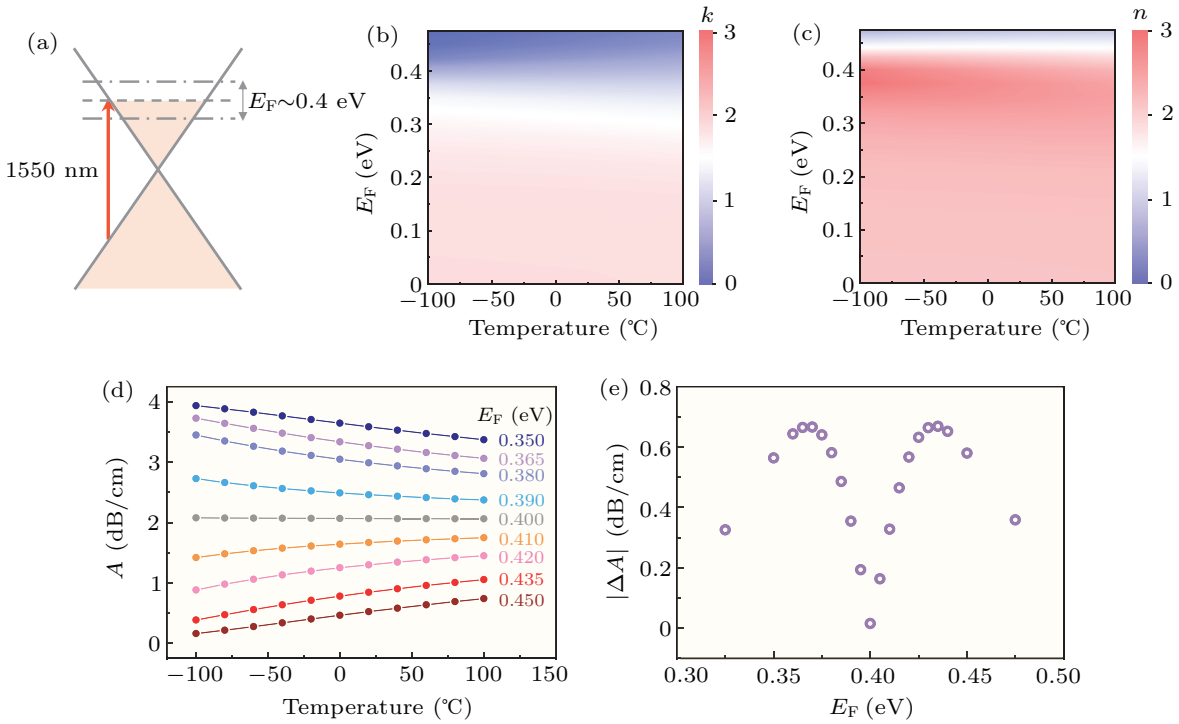


Fig. 3. Sensitivity enhancement of the Gr-PCF temperature sensor by modulating E_F. (a) The simplified electrical band diagram of graphene with E_F adjusted around 0.4 eV and 1550 nm input light. The imaginary part (b) and the real part (c) of graphene complex refractive index with different E_F and temperatures. (d) Transmission attenuation in Gr-PCF with temperature under different E_F around 0.4 eV region. (e) The $|\Delta A|$ (difference of light attenuations between temperatures of −100 °C and 100 °C) change with different E_F around 0.4 eV, showing a dip value at $E_F = 0.4$ eV and two peak values at $E_F = 0.365$ eV and $E_F = 0.435$ eV. The transmission attenuation at $E_F = 0.435$ eV is much lower than that at $E_F = 0.365$ eV (d).

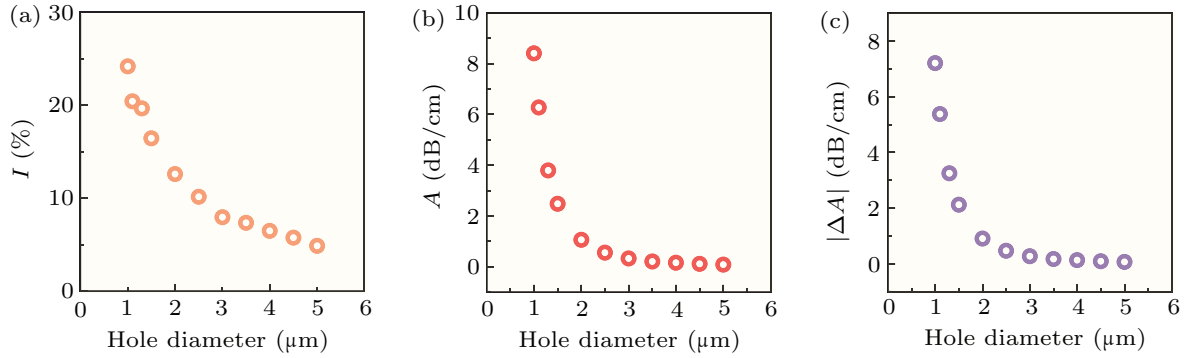


Fig. 4. Sensitivity enhancement by optimizing Gr-PCF structure. (a), (b) The dependence of normalized intensity I at graphene film regime (a) and transmission attenuation A (b) on air-hole diameter at $E_F = 0.435$ eV and 0 °C. Both I and A show an obvious decreasing with hole diameter increasing. (c) The change of $|\Delta A|$ with different hole diameters, exhibiting an evident change from ~ 7.2 dB/cm to ~ 0.07 dB/cm with hole diameter increasing and the sensitivity of ~ 0.036 dB/(cm·°C) for 1 μm hole diameter. The endless single mode transmission property is kept at different hole diameters and pitches.

In addition, the sensor sensitivity is also related to the strength of light–matter interaction in Gr-PCF, which can be improved by optimizing the PCF structure.[42] The performance of sensitivity with different PCF structures is studied on the condition of $E_F = 0.435$ eV, meanwhile, the endless single mode transmission property is kept by elaborately designing the sizes of the hole diameter and pitch.[36] With the Φ reduced from 5 μm to 1 μm and the temperature of 0 °C, the normalized intensity I at graphene film regime of Gr-PCF shows a strong enhancement from ~ 4.9% to ~ 24.2% (Fig. 4(a)). Considering influences of both the light intensity change at the innermost graphene position and the given graphene absorption, the transmission attenuation also shows an increasing trend with Φ changing from 5 μm to 1 μm (Fig. 4(b)). Furthermore, the difference of attenuations ($|\Delta A|$, between the temperatures of −100 °C and 100 °C) demonstrates an obvious enhancement with reducing Φ (Fig. 4(c)), which indicates temperature sensitivity of $\sim 3.6 \times 10^{-2}$ dB/(cm·°C) with $\Phi = 1$ μm, ~ 10 times improvement than that of conventional PCF with $\Phi = 2.22$ μm (Fig. 3(e)). Overall, the decrease of hole diameter in PCF leads to the enhanced light–graphene interaction, and results in dramatically increased sensitivity.

In summary, a highly sensitive temperature fiber sensor based on Gr-PCF with the intact transmission mode is proposed theoretically by modulating E_F and optimizing the PCF structure. With E_F ~ 0.435 eV (35 meV higher than the half

energy of the incident photon), the sensitivity can be enhanced by four orders of magnitudes to $\sim 3.34 \times 10^{-3}$ dB/(cm·°C) with a relatively low transmission attenuation. Furthermore, with the hole diameter optimized to 1 μm, the sensitivity can be improved to ~ 0.036 dB/(cm·°C), which demonstrates a huge potential in highly sensitive temperature sensors. Our strategy provides a new way for the design of high performance all-fiber temperature sensors targeting next-generation optical fiber applications. Furthermore, considering the excellent properties of various nanomaterials such as sufficient volume, high catalytic activity, specific adsorption capacity and remarkable electrocatalytic property,[43–45] these nanomaterials have demonstrated enormous potential to make up for the shortages of intrinsic graphene in the mentioned aspects and be integrated with PCF to target for broadening types or functions of sensors with high performance.

References

[1] Kaminow I P, Li T and Willner A E 2008 *Optical Fiber Telecommunications V A*, 5th edn. (Burlington: Academic) pp. 1–21
[2] Knight J C 2003 *Nature* **424** 847
[3] Russell P 2003 *Science* **299** 358
[4] Tong L M, Gattass R R, Ashcom J B, He S L, Lou J Y, Shen M Y, Maxwell I and Mazur E 2003 *Nature* **426** 816
[5] Giallorenzi T G, Bucaro J A, Dandridge A, Sigel G H, Cole J H, Rashleigh S C and Priest R G 1982 *IEEE J. Quantum Electron.* **18** 626
[6] Lee B 2003 *Opt. Fiber Technol.* **9** 57
[7] Dragic P, Hawkins T, Foy P, Morris S and Ballato J 2012 *Nat. Photon.* **6** 627
[8] Bhatia V and Vengsarkar A M 1996 *Opt. Lett.* **21** 692
[9] Starodumov A N, Zenteno L A, Monzon D and DeLaRosa E 1997 *Appl. Phys. Lett.* **70** 19
[10] Li E B, Wang X L and Zhang C 2006 *Appl. Phys. Lett.* **89** 091119
[11] Markos C, Travers J C, Abdolvand A, Eggleton B J and Bang O 2017 *Rev. Mod. Phys.* **89** 045003
[12] Cao Z X, Yao B C, Qin C Y, Yang R, Guo Y H, Zhang Y F, Wu Y, Bi L, Chen Y F, Xie Z D, Peng G D, Huang S W, Wong C W and Rao Y J 2019 *Light Sci. Appl.* **8** 109
[13] Lou J Y, Wang Y P and Tong L M 2014 *Sensors* **14** 5823
[14] Geim A K and Novoselov K S 2007 *Nat. Mater.* **6** 183
[15] Castro Neto A H, Guinea F, Peres N M R, Novoselov K S and Geim A K 2009 *Rev. Mod. Phys.* **81** 109
[16] Novoselov K S, Geim A K, Morozov S V, Jiang D, Katsnelson M I, Grigorieva I V, Dubonos S V and Firsov A A 2005 *Nature* **438** 197
[17] Wang F, Zhang Y B, Tian C S, Girit C, Zettl A, Crommie M and Shen Y R 2008 *Science* **320** 206
[18] Bonaccorso F, Sun Z, Hasan T and Ferrari A C 2010 *Nat. Photon.* **4** 611
[19] Xia F N, Mueller T, Lin Y M, Valdes-Garcia A and Avouris P 2009 *Nat. Nanotechnol.* **4** 839
[20] Romagnoli M, Sorianello V, Midrio M, Koppens F H L, Huyghebaert C, Neumaier D, Galli P, Templ W, D'Errico A and Ferrari A C 2018 *Nat. Rev. Mater.* **3** 392
[21] Balandin A A, Ghosh S, Bao W Z, Calizo I, Teweldebrhan D, Miao F and Lau C N 2008 *Nano Lett.* **8** 902
[22] Gan X T, Shiue R J, Gao Y D, Meric I, Heinz T F, Shepard K, Hone J, Assefa S and Englund D 2013 *Nat. Photon.* **7** 883
[23] Liu Y D, Wang F Q, Wang X M, Wang X Z, Flahaut E, Liu X L, Li Y, Wang X R, Xu Y B, Shi Y and Zhang R 2015 *Nat. Commun.* **6** 8589
[24] Falkovsky L 2008 *J. Phys.: Conf. Ser.* **129** 012004
[25] Gusynin V P, Sharapov S G and Carbotte J P 2007 *J. Phys.: Condens. Matter* **19** 026222
[26] Hanson G W 2008 *J. Appl. Phys.* **103** 064302
[27] Vakil A and Engheta N 2011 *Science* **332** 1291
[28] Khalaf A L, Mohamad F S, Rahman N A, Lim H N, Paiman S, Yusof N A, Mahdi M A and Yaacob M H 2017 *Opt. Mat. Express* **7** 1858
[29] Luo J J, Liu G S, Zhou W J, Hu S Q, Chen L, Chen Y F, Luo Y H and Chen Z 2020 *J. Mater. Chem. C* **8** 12893
[30] Sridevi S, Vasu K S, Asokan S and Sood A K 2016 *Opt. Lett.* **41** 2604
[31] Zhang J, Liao G Z, Jin S S, Cao D, Wei Q S, Lu H H, Yu J H, Cai X, Tan S Z, Xiao Y, Tang J Y, Luo Y H and Chen Z 2014 *Laser Phys. Lett.* **11** 035901
[32] Sun Q Z, Sun X H, Jia W H, Xu Z L, Luo H P, Liu D M and Zhang L 2016 *IEEE Photon. Tech. Lett.* **28** 383
[33] Chu R, Guan C Y, Bo Y T, Shi J H, Zhu Z, Li P, Yang J and Yuan L B 2019 *IEEE Photon. Tech. Lett.* **31** 553
[34] Horng J, Balch H B, McGuire A F, Tsai H Z, Forrester P R, Crommie M F, Cui B X and Wang F 2016 *Nat. Commun.* **7** 13704
[35] Chen K, Zhou X, Cheng X, Qiao R X, Cheng Y, Liu C, Xie Y D, Yu W T, Yao F R, Sun Z P, Wang F, Liu K H and Liu Z F 2019 *Nat. Photon.* **13** 754
[36] Nielsen M D and Mortensen N A 2003 *Opt. Express* **11** 2762
[37] Liu M, Yin X, Ulin-Avila E, Geng B, Zentgraf T, Ju L, Wang F and Zhang X 2011 *Nature* **474** 64
[38] Bao Q L, Zhang H, Wang B, Ni Z H, Lim C H Y X, Wang Y, Tang D Y and Loh K P 2011 *Nat. Photon.* **5** 411
[39] Li W, Chen B G, Meng C, Fang W, Xiao Y, Li X Y, Hu Z F, Xu Y X, Tong L M, Wang H Q, Liu W T, Bao J M and Shen Y R 2014 *Nano Lett.* **14** 955
[40] Zuo Y G, Yu W T, Liu C, Cheng X, Qiao R X, Liang J, Zhou X, Wang J H, Wu M H, Zhao Y, Gao P, Wu S W, Sun Z P, Liu K H, Bai X D and Liu Z F 2020 *Nat. Nanotechnol.* **15** 987
[41] Kittel C and Kroemer H 1971 *Thermal Physics*, 2nd edn. (San Francisco: W. H. Freeman) pp. 189–191
[42] Cheng X, Zhou X, Tao L Y, Yu W T, Liu C, Cheng Y, Ma C J, Shang N Z, Xie J, Liu K H and Liu Z F 2020 *Nanoscale* **12** 14472
[43] Liu J, Jiang X T, Zhang R Y, Zhang Y, Wu L M, Lu W, Li J Q, Li Y C and Zhang H 2019 *Adv. Funct. Mater.* **29** 1807326
[44] Yang S, Liu Y L, Chen W, Jin W, Zhou J, Zhang H and Zakharova G S 2016 *Sens. Actuators B Chem.* **226** 478
[45] Wan P B, Wen X M, Sun C Z, Chandran B K, Zhang H, Sun X M and Chen X D 2015 *Small* **11** 5409